



The studies of phase relation, microstructure, magnetic transition, magnetocaloric effect in $(\text{Gd}_{1-x}\text{Er}_x)_5\text{Si}_{1.7}\text{Ge}_{2.3}$ compounds

Xiang Chen^{a,b}, Yungui Chen^{a,*}, Yongbai Tang^a

^a School of Materials Science and Engineering, Sichuan University, Chengdu 610065, PR China

^b Department of Physics and Electronic Information Engineering, Neijiang Teachers College, Neijiang 641002, PR China

ARTICLE INFO

Article history:

Received 16 November 2010

Received in revised form 7 June 2011

Accepted 3 July 2011

Available online 23 July 2011

Keywords:

$(\text{Gd}_{1-x}\text{Er}_x)_5\text{Si}_{1.7}\text{Ge}_{2.3}$ compounds

Curie temperatures

Magnetic transition

Magnetocaloric effect

ABSTRACT

The phase relation, microstructure, Curie temperatures (T_C), magnetic transition, and magnetocaloric effect of $(\text{Gd}_{1-x}\text{Er}_x)_5\text{Si}_{1.7}\text{Ge}_{2.3}$ ($x=0, 0.05, 0.1, 0.15$, and 0.2) compounds prepared by arc-melting and then annealing at 1523 K (3 h) using purity Gd (99.9 wt.%) are investigated. The results of XRD patterns and SEM show that the main phases in those samples are mono-clinic $\text{Gd}_5\text{Si}_2\text{Ge}_2$ type structure. With increase of Er content from $x=0$ to 0.2 , the values of magnetic transition temperatures (T_C) decrease linearly from 228.7 K to 135.3 K. But the $(\text{Gd}_{1-x}\text{Er}_x)_5\text{Si}_{1.7}\text{Ge}_{2.3}$ compounds display large magnetic entropy near their transition temperatures in a magnetic field of 0–2 T. The maximum magnetic entropy change in $(\text{Gd}_{1-x}\text{Er}_x)_5\text{Si}_{1.7}\text{Ge}_{2.3}$ compounds are 24.56, 14.56, 16.84, 14.20, and 13.22 J/kg K^{−1} with $x=0, 0.05, 0.1, 0.15$, and 0.2 , respectively.

© 2011 Elsevier B.V. All rights reserved.

1. Introduction

Magnetic refrigeration is based on the magnetocaloric effect and is discovered by Warburg in 1881 [1]. It is realized by utilizing the heat releasing or absorbing of a magnetic material due to a magnetic field change ΔH . For a long time, the main application of the magnetic refrigeration is to attain very low temperatures. Until the discovery of giant magnetocaloric effect (GMCE) in $\text{Gd}_5\text{Si}_2\text{Ge}_2$ and related $\text{Gd}_5(\text{Si}_x\text{Ge}_{1-x})_4$ compounds around room temperature in 1997 [2–6], the possibility of magnetic refrigerants for room temperature applications has become plausible. The giant magnetocaloric effect (GMCE) in $\text{Gd}_5\text{Si}_2\text{Ge}_2$ is associated with a first-order magnetic transition accompanied with a structural phase transition from an orthorhombic low temperature phase (space group Pnma) to a monoclinic high temperature phase (space group P112₁/a). The discovery of GMCE in $\text{Gd}_5\text{Si}_2\text{Ge}_2$ brought the abundant studies for the room temperature magnetic refrigerant materials with a first-order magnetic transition, such as $\text{LaFe}_{13-x}\text{Si}_x$, $\text{MnFeP}_{1-x}\text{As}_x$, and $\text{MnAs}_{1-x}\text{Sb}_x$ [7–13]. It is a milestone in developing room temperature magnetic refrigerant materials. In addition, it also brought the studies on other members of the $\text{Re}_5(\text{Si}_{1-x}\text{Ge}_x)_4$ ($\text{Re}=\text{Ce}, \text{Pr}, \text{Sm}, \text{Tb}, \text{Dy}, \text{Er}, \text{Ho}, \text{Y}$) family. The result indicates that there are diverse natures due to their different physical properties [14–16]. Firstly, different $\text{Re}_5\text{Si}_2\text{Ge}_2$ compounds have different crystal structures. The $\text{Sm}_5\text{Si}_2\text{Ge}_2$ and $\text{Tb}_5\text{Si}_2\text{Ge}_2$ compounds are $\text{Gd}_5\text{Si}_2\text{Ge}_2$ -type monoclinic structure [17,18]. $\text{Pr}_5\text{Si}_2\text{Ge}_2$ is $\text{Gd}_5\text{Si}_2\text{Ge}_2$ -type mono-

clinic structure under 4 K, or it is ZrSi_4 structure [19]. $\text{Ce}_5\text{Si}_2\text{Ge}_2$ is orthorhombic ZrSi_4 structure [20]. The $\text{Re}_5\text{Si}_2\text{Ge}_2$ ($\text{Re}=\text{Dy}, \text{Er}, \text{Ho}, \text{Y}$) compounds are Sm_5Ge_4 structure. But they are $\text{Gd}_5\text{Si}_2\text{Ge}_2$ -type monoclinic structure when $2.6 \leq x \leq 3.2$, $0.35 \leq x \leq 3.8$, $3 \leq x \leq 3.4$, and $4 \leq x \leq 3.5$, respectively [21–25]. $\text{Yb}_5(\text{Si}_{1-x}\text{Ge}_x)_4$ is Gd_5Si_4 structure [26]. Secondly, part $\text{Re}_5(\text{Si}_{1-x}\text{Ge}_x)_4$ compounds also show the giant magnetocaloric effect. $\text{Tb}_5\text{Si}_2\text{Ge}_2$ shows that a magnetic field induced transition occurs near about 110 K and a large MCE with the same origin as that in $\text{Gd}_5\text{Si}_2\text{Ge}_2$ compound [17]. The Er_5Si_4 compound also has the character of a first-order magnetic transition as in $\text{Gd}_5\text{Si}_2\text{Ge}_2$ [25].

Rare earth elements substitute for Gd in $\text{Gd}_5(\text{Si}_x\text{Ge}_{1-x})_4$ compounds have been studied according to the some physical and chemic comparability between different rare earth elements. The small amount substitution of Tb for Gd in $\text{Gd}_5\text{Si}_{1.72}\text{Ge}_{2.28}$ compound decreased the Curie temperature, but the maximum magnetic entropy change in a magnetic field of 0–2.0 T for the $(\text{Gd}_{0.94}\text{Tb}_{0.06})_5\text{Si}_{1.72}\text{Ge}_{2.28}$ alloy reaches 25.13 J/kg K^{−1} [27]. The substitution of Dy or Y for Gd decreased the Curie temperature and the maximum magnetic entropy change in $\text{Gd}_5\text{Si}_2\text{Ge}_2$ compound [28,29]. The studies of $\text{Gd}_{5-z}\text{Re}_z(\text{Si}_x\text{Ge}_{1-x})_4$ ($\text{Re}=\text{Er}, \text{Ce}, \text{Pr}, \text{Sm}, \text{Dy}, \text{Er}, \text{or Ho}$) are few. In this work, the phase relation, microstructure, Curie temperatures (T_C), magnetic transition, and magnetocaloric effect of $(\text{Gd}_{1-x}\text{Er}_x)_5\text{Si}_{1.7}\text{Ge}_{2.3}$ ($x=0, 0.05, 0.1, 0.15$, and 0.2) compounds were investigated.

2. Experimental techniques

The $(\text{Gd}_{1-x}\text{Er}_x)_5\text{Si}_{1.7}\text{Ge}_{2.3}$ ($x=0, 0.05, 0.1, 0.15$, and 0.2) compounds with nominal composition were prepared by arc

* Corresponding author. Tel.: +86 28 85405670; fax: +86 28 85407335.
E-mail address: ygchen60@yahoo.com.cn (Y. Chen).

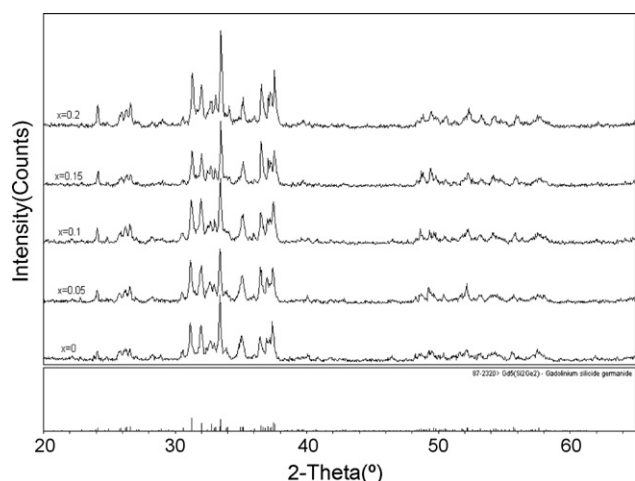


Fig. 1. XRD pattern of $(\text{Gd}_{1-x}\text{Er}_x)_5\text{Si}_{1.7}\text{Ge}_{2.3}$ compounds.

melting under the protection of high purity argon atmosphere (99.999 wt.%). The purities of raw materials Gd, Er, Si and Ge are 99.9 wt.%, 99.9 wt.%, 99.9999 wt.% and 99.9999 wt.%, respectively. The compound buttons were re-melted five times to ensure homogeneity. The as-cast compounds were annealed at 1523 K (3 h) in a molybdenum wire furnace of 3×10^{-3} Pa vacuum, followed by furnace cooling down to room temperature. The phase purity and crystal structures were determined by powder X-ray diffraction (XRD) using Cu (K_α) radiation. Scanning electron microscope (SEM) was carried by Hitachi-S-3400N. Magnetic measurements were performed using a vibrating-sample magnetometer (VSM, Lakeshore 7410). The Curie temperatures (T_C) are determined from the minima of dM/dT of the M - T curves and were measured in an applied magnetic field of $H = 0.02$ T. The isothermal magnetization curves were measured in a temperature range of 150–300 K, and in a magnetic field of 0–2 T. The magnetic entropy changes $\Delta S_M(T, H)$ were calculated from isothermal magnetization curves (M - H curves) in the vicinity of the Curie temperature using the thermodynamic Maxwell relation according to Eq. (1) [30]. For magnetization measured at discrete field and temperature intervals, the magnetic entropy change defined in Eq. (1) can be approximated by Eq. (2) [31].

$$\Delta S_M(T, H) = \int_0^H \left(\frac{\partial M}{\partial T} \right)_H dH \quad (1)$$

$$\Delta S_M(T, H) = \frac{1}{\Delta T} \left[\int_0^H M(T + \Delta T, H) dH - \int_0^H M(T, H) dH \right] \quad (2)$$

3. Results and discussion

Fig. 1 shows the X-ray diffraction (XRD) patterns of the $(\text{Gd}_{1-x}\text{Er}_x)_5\text{Si}_{1.7}\text{Ge}_{2.3}$ compounds collected at room temperature with $x = 0, 0.05, 0.1, 0.15$, and 0.2 , respectively. By analyzing and indexing the X-ray diffraction patterns, one can find that the main phases are monoclinic $\text{Gd}_5\text{Si}_2\text{Ge}_2$ structure in those samples. The main diffraction peaks of the $\text{Gd}_5\text{Si}_2\text{Ge}_2$ structure phase have obvious shift to high angle with the increase of Er content. This is a signature of lattice contraction. It attributes to the radius of Er (1.67 Å) is smaller than that of Gd (1.72 Å). Fig. 2 is the SEM micrographs of the $(\text{Gd}_{1-x}\text{Er}_x)_5\text{Si}_{1.7}\text{Ge}_{2.3}$ compounds. We can observe that there are the regular line microstructures in five compounds, which have been observed in Gd_5Si_4 , $\text{Gd}_5\text{Si}_2\text{Ge}_2$, and Gd_5Ge_4 single crystal alloys [32–34]. The column cellular grains and cellular walls are very clear, and some fine lines in gray matrix basic phase in microstructures. According to the analy-

sis of SEM and EDS of $\text{Gd}_5(\text{Si}_{1-x}\text{Ge}_x)_4$ compounds, Meyers et al. thought that the regular line microstructure is the Widmanstätten $\text{Gd}_5(\text{Si,Ge})_3$ phase [33]. From Fig. 2, one can find that the amounts of regular line microstructure occupy large volume proportion, but the characteristic peaks of $\text{Gd}_5(\text{Si,Ge})_3$ phase cannot be observed in XRD patterns. In addition, the EDS analysis of $(\text{Gd}_{1-x}\text{Er}_x)_5\text{Si}_{1.7}\text{Ge}_{2.3}$ shows that the total atom proportion of Si and Ge are 53.66%, 50.80%, 49.04% in regular line microstructures with $x = 0, 0.1$, and 0.2 , respectively, which are obviously higher than 37.5 at% in $\text{Gd}_5(\text{Si,Ge})_3$ phase. According to the EDS result of $(\text{Gd}_{0.8}\text{Er}_{0.2})_5\text{Si}_{1.7}\text{Ge}_{2.3}$ compound, as shown in Table 1, the compositions of regular line microstructure phase is close to that of the GdGe -type phase. The gray matrix microstructure, fine lines and the dots in gray matrix phase are both $\text{Gd}_5\text{Si}_2\text{Ge}_2$ -type phase. But the atom atomic percent of four elements in those microstructures are different.

Fig. 3 displays the temperature dependent magnetization of $(\text{Gd}_{1-x}\text{Er}_x)_5\text{Si}_{1.7}\text{Ge}_{2.3}$ compounds measured under 0.02 T in heating process from 100 to 270 K. The Curie temperatures (T_C) can be obtained by the minima in the first derivative of the M - T curves in each sample. According to magnetic theory, the T_C is mainly determined by the exchange interactions between the magnetic atoms. In $(\text{Gd}_{1-x}\text{Er}_x)_5\text{Si}_{1.7}\text{Ge}_{2.3}$ compounds, Si and Ge are nonmagnetic, the Curie temperature is determined by the Gd–Gd, Gd–Er, and Er–Er interactions. From Table 2, one can find that T_C of the $(\text{Gd}_{1-x}\text{Er}_x)_5\text{Si}_{1.7}\text{Ge}_{2.3}$ compounds decrease from 228.7 to 135.3 K with increasing of Er content from $x = 0$ to 0.2 . The decrease of the T_C and the Er content almost shows linear relation, as shown in the inset of Fig. 3. This shows that the Curie temperature is very sensitive to the Er content. The decrease of the Curie temperature in the Er-substituted compound is probably associated with the fact that the Gd–Gd and Gd–Er interactions are much stronger than that of the Er–Er interaction in metal systems. Note that the GdCo_2 compound has a high Curie temperature, $T_C = 405$ K [35], but the ErCo_2 with a low Curie temperature, $T_C = 33$ K [36]. Therefore, the substitution of Er for Gd in the $(\text{Gd}_{1-x}\text{Er}_x)_5\text{Si}_{1.7}\text{Ge}_{2.3}$ compounds results in the decrease of Curie temperature, as observed in previous work on the Gd–Er-based compounds [14]. The lattice contraction and the Gd–Gd interactions reduce with increase of Er content are also the factors of the decrease of T_C . In addition, the M - T curve displays a large slope, and it is a typical symbol of the first-order structural/magnetic transition, which results in a large magnetic entropy change.

The isothermal magnetization curves of different temperatures in the vicinity of the Curie temperature are shown in Fig. 4(a–e). The measurements were performed in field increasing process. In order to check whether the isothermal magnetization process involves magnetic hysteresis, one of the magnetic field dependence of magnetization curves near T_C were measured during up and down magnetic field of 0–2 T. One can find that the M - H curves below T_C exhibit a characteristic ferromagnetic behavior. With increasing temperature above T_C , there is a field-induced metamagnetic transition from the paramagnetic state to the ferromagnetic state in $\text{Gd}_5\text{Si}_{1.7}\text{Ge}_{2.3}$ compound, which is characterized by a step sharp change in the magnetization. The transition disappears in the samples with higher Er content. It indicates that the initiated critical field (H_C) of field-induced IEM transition increases with the increase of Er content in $(\text{Gd}_{1-x}\text{Er}_x)_5\text{Si}_{1.7}\text{Ge}_{2.3}$ compounds. The magnetic hysteresis happens inevitably in magnetic refrigeration materials with a first-order phase transition, and the value of magnetic hysteretic loss is also response to the first-order magnetic transition intensity. For $\text{Gd}_5\text{Si}_{1.7}\text{Ge}_{2.3}$ compound, a large magnetic hysteresis occurs, and the value is 43.44 J/kg near T_C . With the increase of Er content up to $x = 0.2$, the magnetic hysteresis reduces to 3.97 J/kg at 136 K [see Fig. 4(e)], it shows that the first-order magnetic transition from paramagnetic to ferromagnetic state is

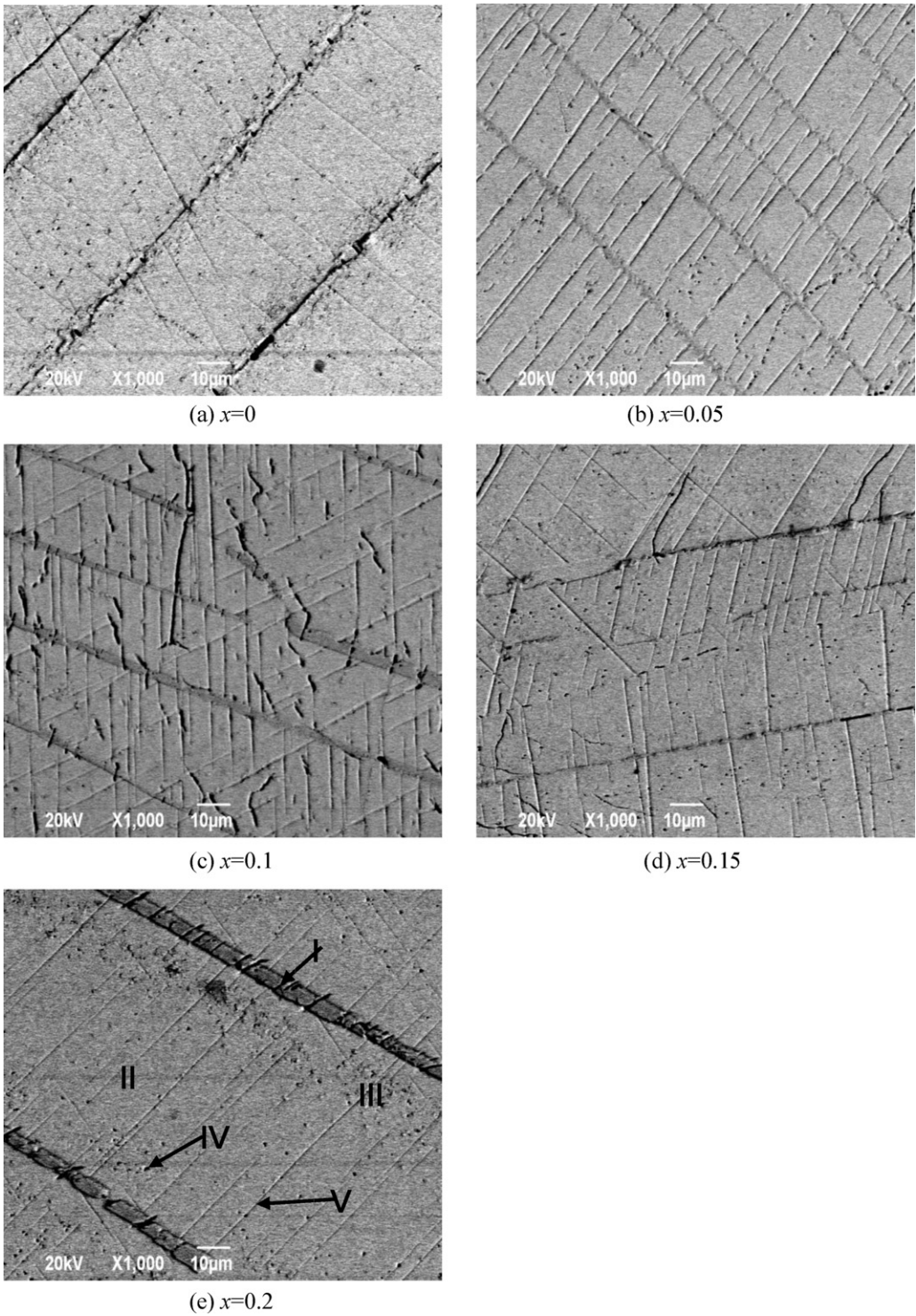


Fig. 2. Backscattered SEM micrographs of $(\text{Gd}_{1-x}\text{Er}_x)_5\text{Si}_{1.7}\text{Ge}_{2.3}$ compounds: (a) $x=0$, (b) $x=0.05$, (c) $x=0.1$, (d) $x=0.15$, (e) $x=0.2$.

weakened with the increase of Er content Fig. 5 shows the Arrott plots of five samples. One can find that negative slopes appear, but the value of negative slope becomes small in turn in those samples. According to the Inoue–Shimizu model [37], negative slopes in Arrott plots often indicate a first order transition and the linear relation in Arrott plot above T_C implies that a second-order magnetic transition occurs. It shows that $(\text{Gd}_{1-x}\text{Er}_x)_5\text{Si}_{1.7}\text{Ge}_{2.3}$ compounds keep the first-order structural/magnetic transition, but the behavior of the first-order magnetic transition becomes feeble with the Er increase.

Table 1
The results of EDS analysis performed on the three phases presents in Fig. 2(e).

	Gd (at%)	Er (at%)	Si (at%)	Ge (at%)	Phase
Region I	42.69	8.26	31.27	17.77	GdGe-type
Region II	44.08	12.73	19.27	23.33	Gd5Si2Ge2-type
Region III	42.71	14.67	20.14	22.51	Gd5Si2Ge2-type
Region IV	41.71	13.47	22.52	22.30	Gd5Si2Ge2-type
Region V	40.16	14.37	22.79	22.67	Gd5Si2Ge2-type

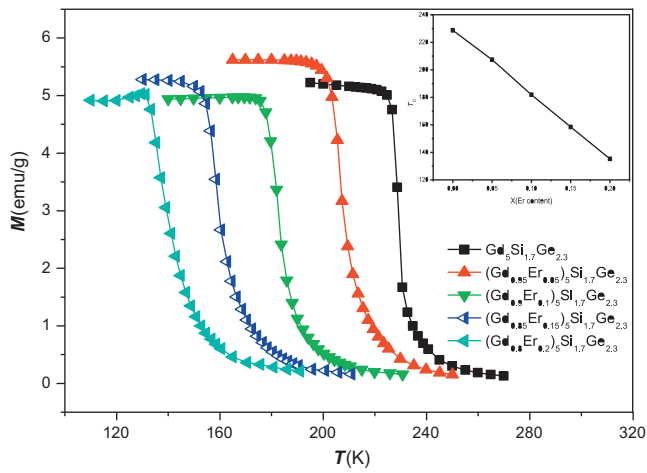


Fig. 3. Temperature dependent magnetization measured of $(\text{Gd}_{1-x}\text{Er}_x)_5\text{Si}_{1.7}\text{Ge}_{2.3}$ compounds under 0.02 T, the inset is the details of T_C of $(\text{Gd}_{1-x}\text{Er}_x)_5\text{Si}_{1.7}\text{Ge}_{2.3}$ dependent Er content.

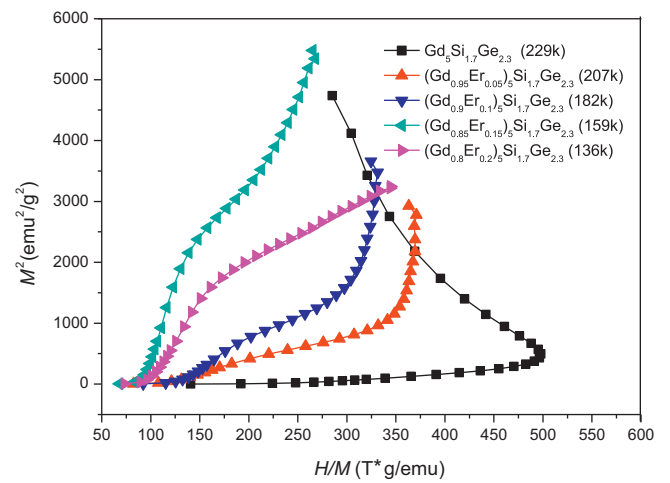


Fig. 5. Arrott plots of $(\text{Gd}_{1-x}\text{Er}_x)_5\text{Si}_{1.7}\text{Ge}_{2.3}$ compounds.

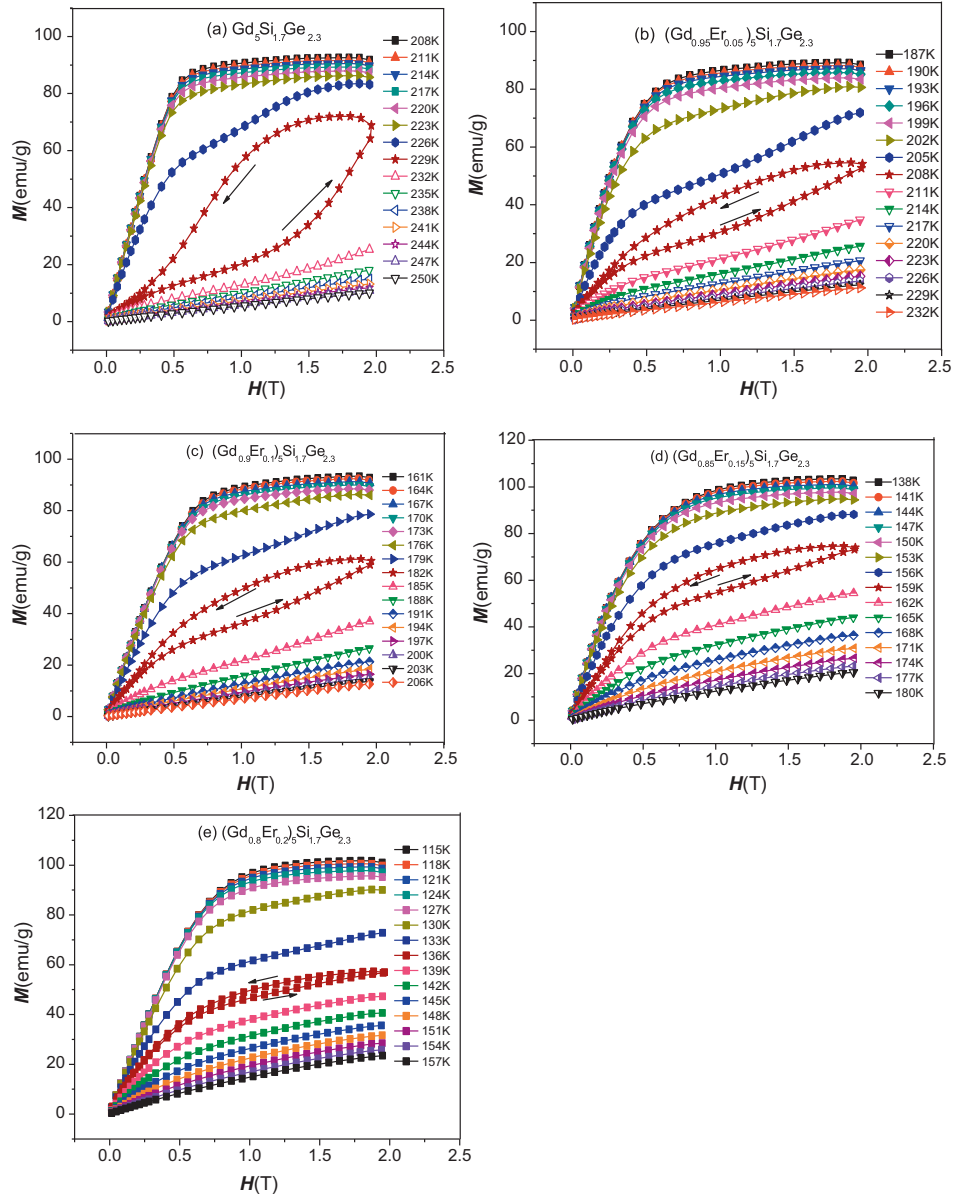


Fig. 4. Magnetization isotherms of $(\text{Gd}_{1-x}\text{Er}_x)_5\text{Si}_{1.7}\text{Ge}_{2.3}$ compounds measured under field of 0–2 T: (a) $x=0$, (b) $x=0.05$, (c) $x=0.1$, (d) $x=0.15$, (e) $x=0.2$.

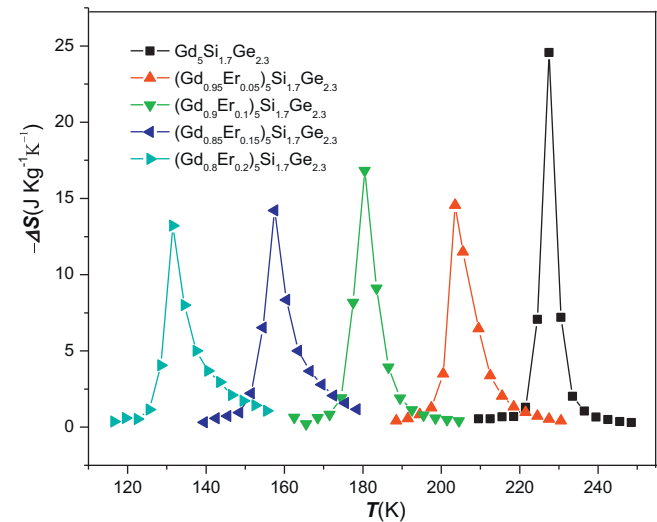


Fig. 6. Magnetic entropy change $\Delta S_M(T,H)$ as functions of temperature of $(\text{Gd}_{1-x}\text{Er}_x)_5\text{Si}_{1.7}\text{Ge}_{2.3}$ compounds.

Table 2
The content of Er, Curie temperature, maximum magnetic entropy changes $\Delta S_{\text{Max}}(T,H)$, magnetic hysteresis loss of $(\text{Gd}_{1-x}\text{Er}_x)_5\text{Si}_{1.7}\text{Ge}_{2.3}$ compounds.

x	T_C	$ \Delta S_{\text{Max}} $ (J/kg K)	Magnetic hysteresis (J/kg)
0.0	228.71	24.56	43.44
0.05	207.34	14.56	15.33
0.1	181.95	16.84	16.39
0.15	158.43	14.20	12.58
0.2	135.26	13.22	3.97

Magnetic entropy change $\Delta S_M(T,H)$ was calculated by Maxwell relation based on the magnetization data. Fig. 6 shows the $\Delta S_M(T,H)$ of $(\text{Gd}_{1-x}\text{Er}_x)_5\text{Si}_{1.7}\text{Ge}_{2.3}$ compounds as functions of temperature. The magnetic entropy changes reach maximum near their first-order structural/magnetic transition temperatures. The maximum magnetic entropy changes with different Er concentration are given in Table 2. In this work, the maximum magnetic entropy change of $(\text{Gd}_{1-x}\text{Er}_x)_5\text{Si}_{1.7}\text{Ge}_{2.3}$ compound is 24.56 J/kg K, which is larger than that of $\text{Gd}_5\text{Si}_{1.72}\text{Ge}_{2.28}$ with no heat treatment using the 3N of Gd raw material in the same magnetic field of 0–2 T and equipment reported in Ref. [27]. It shows that the heat treatment process in this work is beneficial to offset the disadvantage rooting from as-cast $\text{Gd}_5\text{Si}_{4-x}\text{Ge}_x$ compounds with the same raw materials and increase the maximum magnetic entropy changes. Because the introduction of Er weakens the behavior of first-order structural/magnetic transition, the maximum magnetic entropy change decreases with the increase of Er content. The $(\text{Gd}_{0.8}\text{Er}_{0.2})_5\text{Si}_{1.7}\text{Ge}_{2.3}$ compound has a maximum magnetic entropy change of 13.22 J/kg K near its Curie temperature in a magnetic field of 0–2 T. But it is larger than that of Gd under the same applied magnetic field.

4. Conclusions

The $(\text{Gd}_{1-x}\text{Er}_x)_5\text{Si}_{1.7}\text{Ge}_{2.3}$ ($x=0, 0.05, 0.1, 0.15$, and 0.2) compounds are prepared by arc-melting and annealing at 1523 K (3 h) with the purity starting Gd metal of 3N. The main phase remains mono-clinic $\text{Gd}_5\text{Si}_2\text{Ge}_2$ type structure. There are regular line microstructures of GdGe-type phase in five samples, and some

fine lines are observed in gray matrix phases. With the increase of Er content, the lattice shrinks, and the T_C decreases linearly from 228.7 K to 135.3 K. The compounds keep the typical first-order structural/magnetic transition. The maximum magnetic entropy changes in the of $(\text{Gd}_{1-x}\text{Er}_x)_5\text{Si}_{1.7}\text{Ge}_{2.3}$ compounds are 24.56, 14.56, 16.84, 14.20, and 13.22 J/kg K^{−1} with $x=0, 0.05, 0.1, 0.15$, and 0.2 in the applied field change of 0–2.0 T, respectively.

Acknowledgments

The present work was supported by the Key Project of National Natural Science Foundation of China (grant number 50731007) and the National High Technology Research and Development Program of China (grant number 2007AA03Z440).

References

[1] E. Warburg, Ann. Phys. 13 (1881) 141.
[2] V.K. Pecharsky, K.A. Gschneidner Jr., Phys. Rev. Lett. 78 (1997) 4494.
[3] V.K. Pecharsky, K.A. Gschneidner Jr., Appl. Phys. Lett. 70 (1997) 3299.
[4] V.K. Pecharsky, K.A. Gschneidner Jr., J. Alloys Compd. 260 (1997) 98.
[5] W. Choe, V.K. Pecharsky, A.O. Pecharsky, K.A. Gschneidner Jr., V.G. Young Jr., G.J. Miller, Phys. Rev. Lett. 84 (2000) 4617.
[6] L. Morellon, J. Blasco, P.A. Algarabel, M.R. Ibarra, Phys. Rev. B 62 (1022) (2000).
[7] A. Fujita, Y. Akamatsu, K. Fukamichi, J. Appl. Phys. 85 (1999) 4756.
[8] F.X. Hu, B.G. Shen, J.R. Sun, Z.H. Cheng, G.H. Rao, X.X. Zhang, Appl. Phys. Lett. 78 (2001) 3675.
[9] O. Tegus, E. Bruck, K.H.J. Buschow, F.R. de Boer, Nature 415 (2002) 150.
[10] J. Mira, F. Rivadulla, J. Rivas, A. Fondado, T. Guidi, R. Caciuffo, F. Carsughi, P.G. Radaelli, J.B. Goodenough, Phys. Rev. Lett. 90 (2003) 097203.
[11] A. Fujita, S. Fujieda, Y. Hasegawa, K. Fukamichi, Phys. Rev. B. 67 (2003) 104416.
[12] F.X. Hu, M. Ilyn, A.M. Tishin, J.R. Sun, G.J. Wang, Y.F. Chen, F. Wang, Z.H. Cheng, B.G. Shen, J. Appl. Phys. 93 (2003) 5503.
[13] S. Fujieda, A. Fujita, K. Fukamichi, Appl. Phys. Lett. 81 (2002) 1276.
[14] L. Morellon, C. Ritter, C. Magen, P.A. Algarabel, M.R. Ibarra, Phys. Rev. B 68 (2003) 024417.
[15] V.K. Pecharsky, A.O. Pecharsky, Y. Mozharivskiy, K.A. Gschneidner Jr., G.J. Miller, Phys. Rev. Lett. 91 (2003) 207205.
[16] C. Magen, et al., Phys. Rev. B. 74 (2006) 134427.
[17] O. Tegus, O. Dagula, J. Appl. Phys. 91 (2002) 10.
[18] Ahn Kyunghan, V.K. Pecharsky, K.A. Gschneidner Jr., Phys. Rev. 76 (2007) 014415.
[19] H.F. Yang, G.H. Rao, G.Y. Liu, Z.W. Ouyang, W.F. Liu, X.M. Feng, W.G. Chu, J.K. Liang, J. Alloys Compd. 348 (2003) 150.
[20] H. Zhang, Ya. Mudryk, M. Zou, V.K. Pecharsky, K.A. Gschneidner Jr., Y. Long, J. Alloys Compd. 487 (2009) 1–2.
[21] Nirmala, A.V. Morozkin, S.K. Malik, Phys. Rev. B. 75 (2007) 094419.
[22] A.O. Pecharsky, K.A. Gschneidner Jr., V.K. Pecharsky, D.L. Schlager, T.A. Lograsso, Phys. Rev. B. 70 (2004) 144419.
[23] A.M. Pereira, J.B. Sousa, J.P. Araujo, Phys. Rev. B. 77 (2008) 134404.
[24] A.O. Pecharsky, V.K. Pecharsky, K.A. Gschneidner Jr., J. Alloys Compd. 379 (2004) 127.
[25] Y. Mozharivskiy, A.O. Pecharsky, V.K. Pecharsky, G.J. Miller, K.A. Gschneidner Jr., Phys. Rev. B. 69 (2004) 144102.
[26] Ahn Kyunghan, A.O. Tsokol, Yu. Mozharivskiy, K.A. Gschneidner Jr., V.K. Pecharsky, Phys. Rev. B. 72 (2005) 054404.
[27] J.Q. Deng, Y.H. Zhuang, J.Q. Li, K.W. Zhou, J. Alloys Compd. 428 (2007) 28.
[28] R. Nirmalaa, V. Sankaranarayanan, K. Sethupathi, A.V. Morozkin, G. Amish, S.K. Joshi, Malik, J. Magn. Mater. 309 (2007) 212.
[29] C. Vecchini, O. Moze, J. Appl. Phys. 95 (2004) 11.
[30] T. Hashimoto, M. Numasawa, T. Shino, Okada, J. Cryog. 21 (1981) 647.
[31] M. Foldeaki, R. Chahine, T.K. Bose, J. Appl. Phys. 77 (1995) 3528.
[32] J. Szade, G. Skorek, A. Winiarski, J. Cryst. Growth 205 (1999) 289; Z.F. Gu, B. Zhou, J.Q. Li, W.Q. Ao, G. Cheng, J.C. Zhao, Solid State Commun. 141 (2007) 548.
[33] J.S. Meyers, L.S. Chumbley, F. Laabs, A.O. Pecharsky, Scripta Mater. 47 (2002) 509; N.A. de Oliveira, P.J. von Ranke, J. Magn. Mater. 264 (2003) 55.
[34] F. Hao, C. Yungui, T. Mingjing, Z. Tiebang, Acta Mater. 53 (2005) 2377; J. Inoue, M. Shimizu, J. Phys. F 12 (1982) 1811.
[35] Z.F. Gu, B. Zhou, J.Q. Li, W.Q. Ao, G. Cheng, J.C. Zhao, Solid State Commun. 141 (2007) 548.
[36] N.A. de Oliveira, P.J. von Ranke, J. Magn. Mater. 264 (2003) 55.
[37] A. Fujita, Y. Akamatsu, K. Fukamichi, J. Appl. Phys. 85 (1999) 4756.